Molecular Crystals and Liquid Crystals

ISSN: 1542-1406 (Print) 1563-5287 (Online) Journal homepage: http://www.tandfonline.com/loi/gmcl20

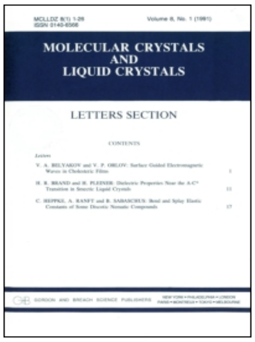

Mesomorphic and DFT studies of terminal ester containing salicylaldimines and their copper (II) complexes

Hemant Kumar Singh, Sachin Kumar Singh, Vijay Kumar, Priyanka Kanth, Kirtika Mishra & Bachcha Singh

To cite this article: Hemant Kumar Singh, Sachin Kumar Singh, Vijay Kumar, Priyanka Kanth, Kirtika Mishra & Bachcha Singh (2017) Mesomorphic and DFT studies of terminal ester containing salicylaldimines and their copper (II) complexes, Molecular Crystals and Liquid Crystals, 643:1, 116-128, DOI: 10.1080/15421406.2016.1263060

To link to this article: http://dx.doi.org/10.1080/15421406.2016.1263060

MOLECULAR CRYSTALS AND LIQUID CRYSTALS
2017, VOL. 643, 116–128
http://dx.doi.org/10.1080/15421406.2016.1263060

Taylor & Francis
Taylor & Francis Group

Mesomorphic and DFT studies of terminal ester containing salicylaldimines and their copper (II) complexes

Hemant Kumar Singh, Sachin Kumar Singh, Vijay Kumar, Priyanka Kanth, Kirtika Mishra, and Bachcha Singh

Department of Chemistry (Centre of Advanced Studies), Institute of Science, Banaras Hindu University, Varanasi, India

ABSTRACT
In this article, we report synthesis and characterization of a novel homologous series of butyl 4-(4′-(alkoxy)-2-hydroxybenzylideneamino) benzoates, C_nLH (n = 6, 8, 10, 12, 14, 16) and their copper(II) complexes. The mesomorphic properties of these compounds were investigated by differential scanning calorimetry (DSC), polarizing optical microscopy (POM) and powder X-ray diffraction (XRD) studies. The ligands and their copper(II) complexes exhibit wide range of enantiotropic smectic A mesophase as confirmed by their typical optical texture under polarizing microscope. Thermal stability of the compounds is determined by thermo gravimetric analyses. DFT calculations have been performed using GAUSSIAN-09 program at B3LYP level to obtain the stable electronic structure of the ligand and its copper(II) complex.

KEYWORDS
Copper complexes; density functional theory; metallomesogens; salicylaldimine; structure–property correlation

Introduction

The diverse mesogenic behaviour of liquid crystals (LCs) makes LCs suitable for application in various fields and because of wide applications such as selective reflection of light and ferroelectricity, LCs are one of the most studied systems in material science [1]. The salicylaldimine core is recognized as a good mesogenic core in liquid crystalline materials because the azomethine linkage is stabilized by intra-molecular hydrogen bonding, and it has the ability to coordinate metals [2–3]. The incorporation of transition metals into liquid crystals has led to the study of interesting magnetic, electronic and optical properties in mesomorphic materials. Metallomesogens (metal containing liquid crystals) have gained attention because of their unusual geometries and novel properties such as colour, paramagnetism, fluidity, large birefringence, polarizability, spin cross-over, ferroelectricity, photo refractivity, nonlinear optical characteristics, large magnetic anisotropy, and luminescent mesophases [4]. Since the metallomesogens are achieved through changes of molecular conformation, shape, and structure, their physico-chemical properties can be tuned by the choice of metal ions, substituents, and position of substituents on core moieties. In 1984 Ovchinnikov and coworkers were first to exploit the coordination possibilities of salicylideneanilines and they reported the first imino-derived metallomesogens [5–8]. He found that alkyl chain length is deciding factor for the mesophase formation. When the alkyl chain length is short at both ends, the compounds are

CONTACT Bachcha Singh ✉ bsinghbhu@rediffmail.com Department of Chemistry (Centre of Advanced Studies), Institute of Science, Banaras Hindu University Varanasi 221005, India.
Color versions of one or more of the figures in the article can be found online at www.tandfonline.com/gmcl.

non mesogenic in nature while by elongation of one alkyl chain length smectic A mesophase is observed. In addition, a smectic C phase is observed for cases where both alkoxy tails are long [9]. We have replaced one chain by $-CO_2CH_2CH_2CH_2CH_3$ group to understand the effect of polar group on mesogenic property. For more advanced applications of LC phases, it is necessary to understand more deeply the structure–property correlation as well as molecular origin of mesophases and phase behaviour. In continuation of the earlier work [10] on systematic structural studies of salicylaldimine mesogenic organic Schiff-bases and their Cu(II) complexes, we now report here the synthesis and mesogenic properties of butyl 4-(4′-(alkoxy)-2-hydroxybenzylideneamino)benzoate and their Cu(II) complexes.

Result and discussion

Synthesis

The synthetic route for preparation of salicylaldimine based ligands and their copper (II) complexes is outlined in Scheme 1. Alkylation of 2,4-dihydroxybenzaldehyde with alkyl bromide in 2-butanone using potassium hydrogen carbonate leads to formation of 4-(alkoxy)-2-hydroxybenzaldehyde. The Schiff base was obtained by the condensation of butyl 4-aminobenzoate with appropriate aldehydes in refluxing ethanol. The metal complexes were prepared by reaction of butyl 4-(4′-(alkoxy)-2-hydroxybenzylideneamino)benzoate with copper(II) acetate in refluxing ethanol. The copper complexes were then isolated as brown solid, by recrystallization from absolute ethanol in good yield. All the ligands and their copper(II) complexes were characterized by standard spectroscopic techniques. The experimental procedures, synthesis of the intermediates and analytical data are described in experimental section.

Mesomorphic behavior

The mesomorphic behaviour of the ligands and their Cu(II) complexes were studied by combining thermo gravimetric analyses (TGA), differential scanning calorimetry (DSC), polarised optical microscopy (POM) and XRD studies (in selected cases). Transition temperatures together with associated enthalpy and entropy changes are given in Tables 1 and 2.

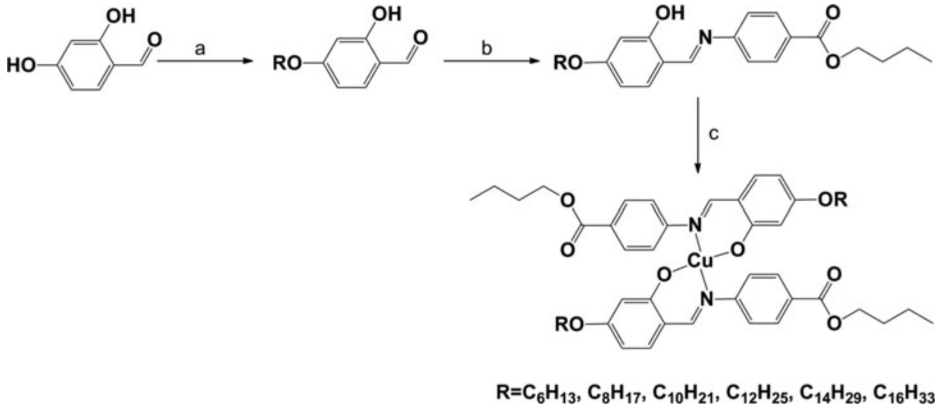

Scheme 1. *Reactions and reagents:* (a) RBr (1.0 equiv.), potassium hydrogen carbonate (1.1 equiv.), refluxing in 2-butanone, 30 h (b) butyl 4-aminobenzoate (1.0 equiv.), acetic acid (4–5 drops), refluxing in ethanol, 4 h (c) $Cu(OAc)_2.H_2O$ (0.5 equiv.), stirring, 4 h.

Table 1. Thermal transitions and corresponding thermodynamic parameters.

Compd	Heating	Cooling
	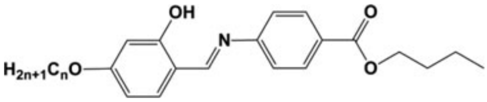 T,°C [ΔH, kJ/mol; ΔS, J/(mol K)]	
1a	Cr 79.20 (33.73; 95.73) Cr′ 96.35 (21.19; 57.37) SmA 104.26 (6.53; 17.31) i	i 101.87 (−6.15; −16.39) SmA 64.03 (−29.93; −88.77) Cr
1b	Cr 58.00 (26.94; 81.34) Cr′ 71.84 (18.30; 53.03) SmA 103.91 (5.27; 13.98) i	i 103.02 (−5.23; −13.89) SmA 53.04 (−15.99; −49.01) Cr
1c	Cr 62.19 (27.76; 82.77) SmA 102.31 (4.75; 12.65) i	i 99.59 (−2.62; −7.03) SmA 45.43 (−32.84; −103.09) Cr
1d	Cr 63.50 (33.30; 98.92) SmA 101.72 (3.70; 9.89) i	i 97.20 (−3.73; −10.07) SmA 36.68 (− 22.64; −73.07) Cr
1e	Cr 54.72 (23.52; 71.72) SmA 98.27 (8.52; 22.93) i	i 95.69 (−9.43; −25.55) SmA 38.73 (−41.01; −131.50) Cr
1f	Cr 70.70 (49.27; 143.30) SmA 97.38 (5.94; 16.02) i	i 95.57 (−5.33; −14.45) SmA 52.25 (−42.48; −130.56) Cr

Abbreviations: Cr & Cr′ = crystalline state, Sm A = Smectic A mesophase, i = isotropic liquid.

In the series of mesogens, 1b with the octyloxy chain length showed three endothermic peaks at 58.0, 71.8, and 103.9°C, followed by the appearance of two exothermic peaks at 103°C and 53°C (Fig. 1).

POM observations reveal that upon heating from crystal state to 71.8°C, focal conic fan shaped texture corresponding to SmA mesophase emerges, which further transforms to isotropic liquid at 103.9°C. In cooling cycle, POM reveals the same textural observations from 103°C to 53°C. From POM analysis, it is clear that the two peaks observed in DSC heating scan are due to crystal transformation from one state to another (Cr–Cr’ transition); such polymorphism has often been observed in Schiff base-containing compounds [11]. Reheating regenerates the focal conic SmA mesophase with similar pattern; that is, the mesomorphism is enantiotropic (Fig. 2). A similar phase transition with a similar textural pattern is

Table 2. Thermal transitions and corresponding thermodynamic parameters.

Compd	Heating	Cooling
	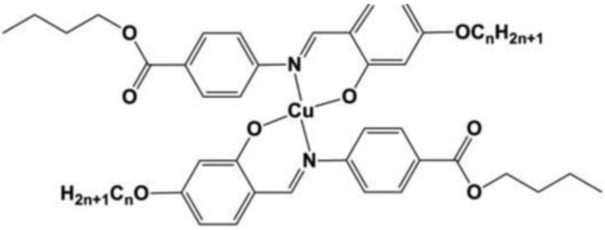 T,°C [ΔH, kJ/mol; ΔS, J/(mol K)]	
2a	Cr 110.69 (17.40; 45.33) Cr′ 169.89 (32.12; 72.45) SmA 174.09 (6.20; 13.86) i	i 171.35 (−8.84; −19.80) SmA 150.23 (−29.23; −68.97) Cr
2b	Cr 93.18 (3.74; 10.20) Cr′ 145.73 (35.28; 84.22) SmA 163.52 (7.76; 17.77) i	i 161.79 (−7.35; −16.89) SmA 106.26 (−30.49; −80.35) Cr
2c	Cr 104.67 (11.71; 30.99) Cr′ 140.86 (29.76; 71.88) SmA 161.89 (9.34; 21.47) i	i 159.69 (−4.75; −10.97) SmA 93.39 (− 19.80; −54.01) Cr
2d	Cr 101.33 (28.39; 75.80) Cr′ 124.11 (33.31; 83.85) SmA 159.10 (7.90; 18.27) i	i 156.32 (−7.41; −17.26) SmA 74.90 (− 22.59; −64.91) Cr
2e	Cr 97.47 (5.63; 15.19) Cr′ 121.59 (22.87;57.94) SmA 153.19 (9.41; 22.07) i	i 148.94 (−6.96; −16.49) SmA 72.82 (− 21.03; −60.79) Cr
2f	Cr 103.56 (28.17; 74.78) Cr′ 110.17 (120.86; 315.29) SmA 148.68 (8.80; 20.84) i	i 147.34 (−8.60; −20.45) SmA 61.62 (− 28.66; −85.61) Cr

Abbreviations: Cr & Cr′ = crystalline state, Sm A = Smectic A mesophase, i = isotropic liquid.

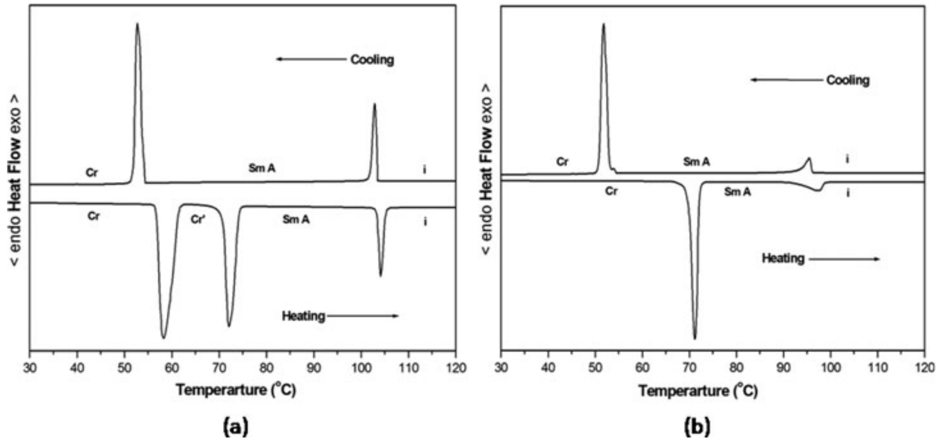

Figure 1. DSC thermogram of (a) butyl 4-(4′-(octyloxy)-2-hydroxybenzylideneamino)benzoate (b) butyl 4-(4′-(hexadecyloxy)-2-hydroxybenzylideneamino)benzoate.

shown by compound 1a. From DSC analysis, we found the two endothermic and two exothermic peaks in compounds 1c–1f. POM analysis reveals that the two endothermic peaks are correspondence to crystal-to-mesophase and mesophase-to-isotropic and in cooling cycle two peaks correspondence to isotropic-to-mesophase and mesophase-to-crystal phase. In the series of butyl 4-(4′-(alkyloxy)-2-hydroxybenzylideneamino)benzoate, the liquid crystal transition temperature decreases from the hexyloxy to tetradecyloxy derivatives and then increases in case of hexadecyloxy derivatives in the heating cycle. In the cooling cycle, the story is quite different as the transition temperature decreases from hexyloxy to hexadecyloxy derivative. Compound 1d and 1e show the SmA mesophase near to room temperature in cooling cycle. On the basis of these observations we can say that moderate chain length of soft alkoxy tails may be assumed as most appropriate to gain good mesophase stability. Transition temperatures of compounds 1a–1f are given in Table 1.

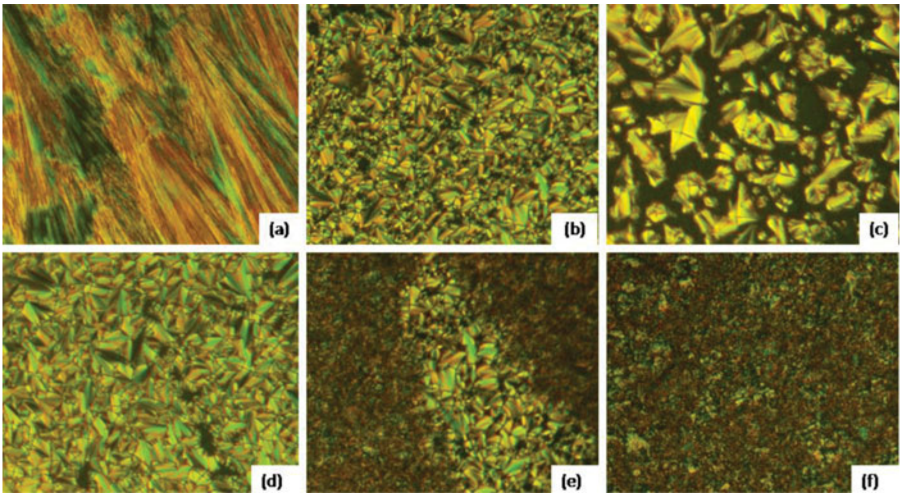

Figure 2. Optical textures of butyl 4-(4′-(dodecyloxy)-2-hydroxybenzylideneamino)benzoate under a polarizing optical microscopy. Heating cycle: (a) crystal phase at 60°C (b) SmA mesophase at 90°C (c) SmA mesophase to isotropic transition at 101°C. Cooling cycle: (d) SmA mesophase at 96°C (e) SmA mesophase to crystal transition at 36°C (f) Crystal phase at 35°C.

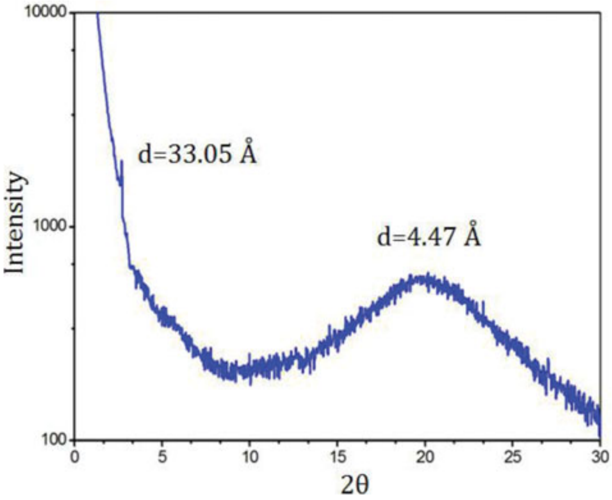

Figure 3. XRD diffractogram at 60°C during the cooling cycle of butyl 4-(4′-(dodecyloxy)-2-hydroxybenzylideneamino)benzoate.

In order to explain the structure of the mesophase, X-ray measurements were performed on unaligned (powder) samples. The XRD experiments were carried out with CuKα ($\lambda = 1.54$ Å) radiation. The samples under investigation were heated slightly above their isotropization temperature and filled into Lindemann capillary tubes and both the ends of the tubes were flame sealed. The XRD patterns for the compound 1d at 60°C are shown in Fig. 3. The diffractograms obtained at different temperatures exhibited similar characteristics; a sharp and intense peak was seen in the small angle region while the wide angle region contained a weak and diffuse peak. XRD patterns with the single, sharp low angle diffuse scattering accompanied by a high-angle diffuse peak is typical of a smectic phase wherein the constituent mesogens, being orientationally aligned, form a layered structure with inter-molecular separation within the smectic layer arising due to the liquid-like positional correlation in the smectic layer.

The copper complexes of the series also exhibit SmA mesophase, but at higher temperature (above 148°C) in comparison to the parent ligands. In the first heating scan of 2b, three sharp peaks appear at 93.2°C, 145.7°C, and 163.5°C. The DSC thermogram recorded in the cooling scan exhibits two distinct peaks at 161.8°C and 106.3°C (Fig. 4). The three peaks observed in heating cycle for this compound define the crystal-to-crystal, crystal-to-mesophase and mesophase-to-isotropic phase transition and two peaks in cooling cycle reveal an isotropic-to-mesophase and mesophase-to-crystal transition. POM observations reveal that upon heating from crystal state to 145.7°C, focal conic texture corresponding to SmA mesophase emerges, which further transforms to isotropic liquid at 163.5°C. In cooling cycle, POM reveals the same textural observations, which emerges from 161.8°C and solidifies at 106.3°C (Fig. 5). A similar phase transition with a similar textural pattern is shown by compound 2a and 2c.

The compound 2d with dodecyloxy chain length shows three endothermic peaks at 101.3°C, 124.1°C, and 159.1°C in the first heating scan and two exothermic peaks at 156.3°C and 74.9°C. Focal conic fan shaped texture of SmA mesophase was observed in both the heating and cooling cycle. Same textural pattern are also found in 2e and 2f. The transition temperature and associated entropy and enthalpy are summarized in Table 2.

The mesophase structures of copper(II) complex, 2d was confirmed by XRD studies of unoriented samples filled in Lindemann capillaries. The XRD pattern at 130°C in the smectic

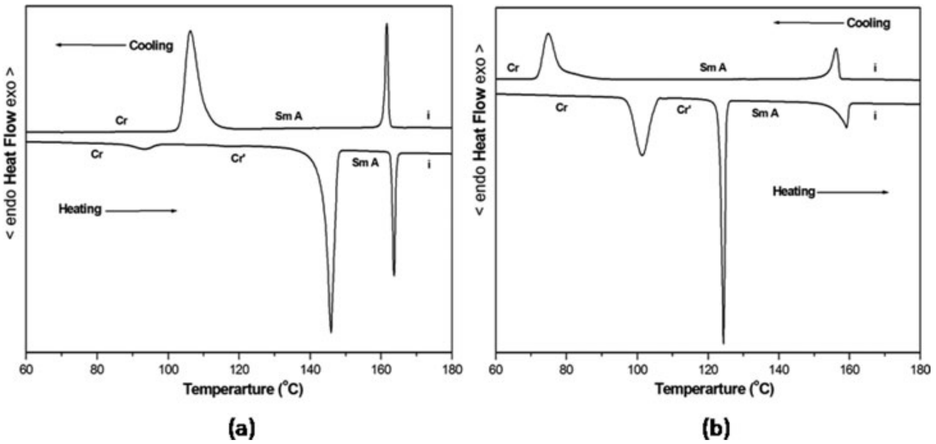

Figure 4. DSC thermogram of (a) copper(II) complex of butyl 4-(4′-(octyloxy)-2-hydroxy benzylideneamino)benzoate (b) copper(II) complex of butyl 4-(4′-(dodecyloxy)-2-hydroxy benzylideneamino) benzoate.

A phase is shown in Fig. 6. Two sharp peaks in the small angle region with d spacings 32.68 Å and 15.85 Å were observed in small angle region while the wide angle region contained diffuse peak at 4.54 Å. These features confirm the mesophase to be SmA in agreement with the POM observations. The wide-angle diffuse peak indicates the fluid-like correlation of the molecules in the layers.

Computational study

The single molecular optimization has been done to investigate the molecular properties using the DFT method. The optimized structures of the ligand and its Cu(II) complex are shown in Fig. 7.

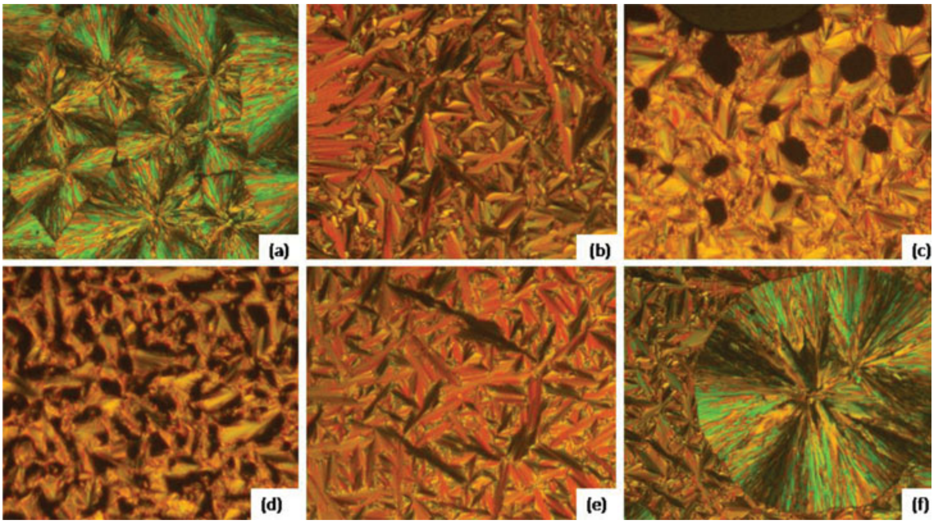

Figure 5. Optical textures of copper(II) complex of butyl 4-(4′-(dodecyloxy)-2-hydroxybenzylide neamino)benzoate under a polarizing optical microscopy. Heating cycle: (a) crystal phase at 112°C (b) SmA mesophase at 140°C (c) SmA mesophase to isotropic transition at 159°C. Cooling cycle: (d) Isotropic to SmA mesophase at 156°C (e) SmA mesophase at 130°C (f) SmA mesophase to crystal transition at 75°C.

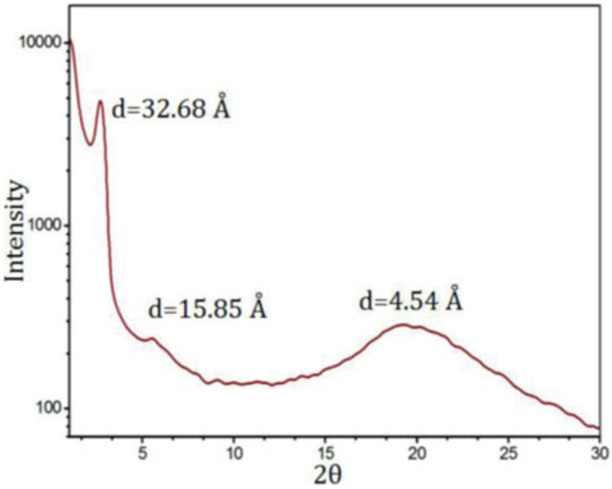

Figure 6. XRD diffractogram at 60°C during the cooling cycle of butyl 4-(4′-(dodecyloxy)-2-hydroxybenzylideneamino)benzoate.

The absence of any imaginary frequency in the calculated vibrational frequencies ensures that the optimized geometry corresponds to a true energy minimum. Some of the selective geometrical parameters of the optimised ligand and its Cu(II) complex, evaluated by density functional theoretical (DFT) calculations at B3LYP/6–311+G (d) basis set for the ligand while for metal complex mixed basis set (6-311+G (d) for C,H, N atoms and LANL2DZ for copper metal) is used, are shown in Table 3.

To investigate the different stable rotational conformers, we have calculated energy by variation of the dihedral angle $C_{10}–N_{12}–C_{16}–C_{17}$ in between 0° and 180° at 10° interval. The relative energy with respect to the optimised structure vs. Dihedral angle is shown in Fig. 8. From this, we see that the most stable conformer for 1c at the potential energy surface is at a dihedral angle of 30° and there is another local minimum at a dihedral angle of 150° with an energy difference of 0.23 kJ/mol. From this, we conclude that most of the molecules prefer to be present in the global minima in solid phase.

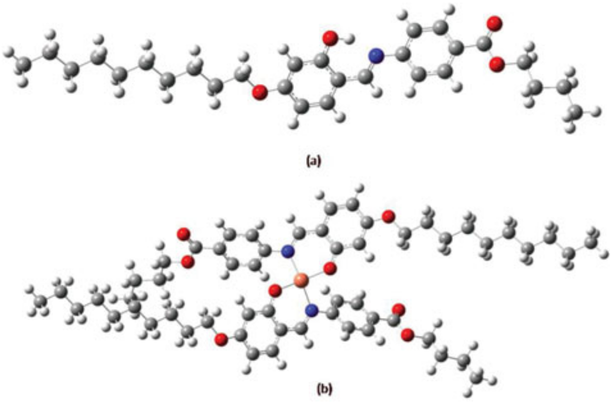

Figure 7. The optimized structure of (a) butyl 4-(4′-(decyloxy)-2-hydroxybenzylideneamino) benzoate and (b) copper(II) complex of butyl 4-(4′-(decyloxy)-2-hydroxy benzylideneamino) benzoate molecule using DFT method.

Table 3. Selected bond lengths and bond angles of copper(II) complex of butyl 4-(4′-(decyloxy)-2-hydroxybenzylideneamino) benzoate.

Structure parameter	Cu-complex[a]
Cu–O(32)	1.93
Cu–O(82)	1.93
Cu–N(12)	2.01
Cu–N(75)	2.01
O(32)– Cu–O(82)	150.68
N(12)– Cu –N(75)	154.79
N(12)–Cu–O(32)	92.97
N(75)–Cu–O(82)	92.96
N(12)–Cu–O(82)	93.69
N(75)–Cu–O(32)	93.04

[a] bond lengths are reported in angstrom (Å) and bond angles in degrees (°).

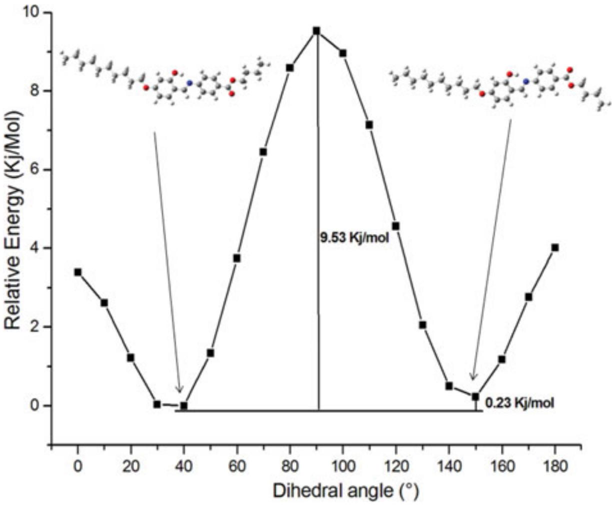

Figure 8. Potential energy vs dihedral angle ($-C_{17}-C_{16}-N_{12}-C_{10}-$) curve of butyl 4-(4′-(decyloxy)-2-hydroxybenzylideneamino)benzoate.

Conclusion

A novel homologous series of butyl 4-(4′-(alkoxy)-2-hydroxybenzylideneamino)benzoates, C_nLH (n = 6, 8, 10, 12, 14, 16) and their copper(II) complexes have been synthesized and the mesomorphic behaviour have been analyzed using DSC, POM, XRD and DFT techniques. All members show SmA mesophase with focal conic textures, having large values of enthalpy and entropy change during the transitions. DFT calculations have been also performed to obtain the stable electronic structure of the ligand and its copper(II) complex. This study will help in exploring further possibilities of the synthesis of thermally stable novel liquid crystalline compounds by variation of nature of substituents at peripheral, lateral positions and density of alkoxy chain length.

Experimental details

Materials

The reagents were purchased from commercial sources and were used as received: 2,4-dihydroxybenzaldehyde, butyl 4-aminobenzoate, 1-bromoalkanes and copper acetate monohydrate are from Aldrich Chemicals, USA. All other solvents and reagents were purchased from Merck. The solvents were dried using standard methods when required [12].

Instrumental

Structural characterization

Structural characterization of the compound was carried out through a combination of CHN analyzer (CE-440 Exeter Analytical CHN analyzer), Infrared spectroscopy (Varian 3100 FT-IR Excalibur series spectrophotometer) using KBr pellets, ^1H and ^{13}C NMR spectra (JEOL FT-NMR AL 300 MHz spectrometer) in $CDCl_3$ using tetramethylsilane as an internal standard, UV-visible spectrometer (UV-1700 Pharma Spec. Shimadzu) in $CHCl_3$ solution.

Thermal analysis

The DSC thermograms were recorded on Mettler Toledo TC 15 TA differential scanning calorimeters at the rate of 5.0°C min^{-1} under nitrogen atmosphere using spec pure grade indium standard and taking samples in close lid aluminium pans. The transition temperatures have been determined from DSC with accuracy of ±0.1°C. Thermo gravimetric analysis (TGA) was performed using a PerkinElmer-STA 6000 apparatus under high purity nitrogen.

Polarized optical microscopic study

The mesophase type was identified by visual comparison with known phase standards using a Nikon Eclipse LV-100 POL polarizing optical microscope (POM) fitted with a hot stage temperature-controlled LTSE 420 heating stage (Linkam Scientific Instruments, Tadworth, Surrey, UK) with temperature controlling accuracy of 0.1 K.

Xray diffraction study

For the temperature-dependent Xray diffraction measurements, a PAN alytical X'Pert PRO MP X-ray diffractometer consisting of a focusing elliptical mirror and a fast high resolution detector (PIXCEL) was employed; the wavelength of the radiation in this case also was 0.15418 nm. The profiles collected using this apparatus were analyzed using Fityk profile fitting software.

Density functional theory (DFT) studies

The GAUSSIAN-09 program package was employed to carry out DFT calculations at the Becke's three parameter functionals and Lee, Yang, and Parr correlation functionals (B3LYP). The internal coordinates of the system, which is used as input for GAUSSIAN-09 program was generated by the GAUSS VIEW 4.1 program [13–24].

Synthesis and analytical data

The starting material 4-(alkoxy)-2-hydroxybenzaldehyde was prepared according to literature procedure [10].

Synthesis of butyl 4-(4′-(hexyloxy)-2-hydroxybenzylideneamino)benzoate, C_6LH (1a)

The ligand, (C_6LH) was prepared by refluxing together an absolute ethanolic solution of 4-(hexyloxy)-2-hydroxybenzaldehyde (1.11 g, 5 mmol) and butyl 4-aminobenzoate (0.97 g, 5 mmol) for 4 h with a few drops (4-5 drops) of acetic acid. The yellow precipitate that formed on cooling was filtered off, washed with cold ethanol and recrystallized from ethanol-chloroform mixture (1/1, v/v). All the other members of the series were prepared in a similar manner.

Yield: 87%. IR (KBr, cm^{-1}): 3410 (−OH), 2956, 2924, 2842 (aliphatic C-H), 1713 (ester, C=O), 1628 (C = N), 1594, 1564 (Ph), 1274, 1238 (OPh); ^{1}H NMR (300 MHz, $CDCl_3$, 25°C) δ_H (ppm): 13.41 (s, 1H, −OH), 8.53 (s, 1H, −CH = N), 8.10 (d, J_1 (H,H) = 8.4 Hz, 2H, $-C_6H_4$), 7.28 (d, J_1 (H,H) = 8.2 Hz, 3H, $-C_6H_4$), 6.48 (d, 2H, $-C_6H_3$), 4.35 (t, 2H, $-OCH_2$), 4.02 (t, 2H, $COOCH_2$), 1.80-1.43 (m, 12H, $-[CH_2]_6$), 1.01 (t, 3H, $-CH_3$), 0.89 (t, 3H, $-CH_3$); ^{13}C NMR (75 MHz, $CDCl_3$, 25°C): δ_c 166.18, 164.10, 164.02, 162.75, 152.43, 133.85, 130.94, 128.10, 120.87, 112.75, 107.90, 101.57, 68.32, 64.85, 31.85, 30.77, 29.53, 29.29, 29.02, 25.95, 22.65, 19.26, 14.08, 13.75; Elemental analyses: calculated for $C_{24}H_{31}NO_4$ (%) C, 72.52; H, 7.86; N, 3.52; Found C, 72.41; H, 7.81; N, 3.54.

Synthesis of butyl 4-(4′-(octyloxy)-2-hydroxybenzylideneamino)benzoate, C_8LH (1b)

Yield: 89%. IR (KBr, cm^{-1}): 3413 (−OH), 2952, 2921, 2852 (aliphatic C-H), 1710 (ester, C=O), 1630 (C = N), 1590, 1561 (Ph), 1273, 1240 (OPh); ^{1}H NMR (300 MHz, $CDCl_3$, 25°C) δ_H (ppm): 13.44 (s, 1H, −OH), 8.53 (s, 1H, −CH = N), 8.09 (d, J_1 (H,H) = 8.4 Hz, 2H, $-C_6H_4$), 7.29 (d, J_1 (H,H) = 8.2 Hz, 3H, $-C_6H_4$), 6.50 (d, 2H, $-C_6H_3$), 4.36 (t, 2H, $-OCH_2$), 4.03 (t, 2H, $COOCH_2$), 1.79-1.45 (m, 16H, $-[CH_2]_8$), 1.01 (t, 3H, $-CH_3$), 0.89 (t, 3H, $-CH_3$); ^{13}C NMR (75 MHz, $CDCl_3$, 25°C): δ_c 166.20, 164.12, 164.03, 162.73, 152.42, 133.83, 130.93, 128.12, 120.89, 112.74, 107.89, 101.56, 68.30, 64.84, 31.87, 30.76, 29.52, 29.28, 29.02, 25.94, 22.65, 19.26, 14.07, 13.74; Elemental analyses: calculated for $C_{26}H_{35}NO_4$ (%) C, 73.38; H, 8.29; N, 3.29; Found C, 73.32; H, 8.25; N, 3.27.

Synthesis of butyl 4-(4′-(decyloxy)-2-hydroxybenzylideneamino)benzoate, C_{10}LH (1c)

Yield: 90%. IR (KBr, cm^{-1}): 3408 (−OH), 2957, 2922, 2848 (aliphatic C-H), 1711 (ester, C=O), 1629 (C = N), 1592, 1564 (Ph), 1276, 1236 (OPh); ^{1}H NMR (300 MHz, $CDCl_3$, 25°C) δ_H (ppm): 13.43 (s, 1H, −OH), 8.52 (s, 1H, −CH = N), 8.09 (d, J_1 (H,H) = 8.4 Hz, 2H, $-C_6H_4$), 7.28 (d, J_1 (H,H) = 8.2 Hz, 3H, $-C_6H_4$), 6.49 (d, 2H, $-C_6H_3$), 4.35 (t, 2H, $-OCH_2$), 4.01 (t, 2H, $COOCH_2$), 1.81-1.43 (m, 20H, $-[CH_2]_{10}$), 1.01 (t, 3H, $-CH_3$), 0.89 (t, 3H, $-CH_3$); ^{13}C NMR (75 MHz, $CDCl_3$, 25°C): δ_c 166.20, 164.10, 164.03, 162.75, 152.42, 133.85, 130.93, 128.10, 120.89, 112.75, 107.89, 101.57, 68.30, 64.85, 31.87, 30.77, 29.52, 29.29, 29.02, 25.94, 22.65, 19.26, 14.07, 13.75; Elemental analyses: calculated for $C_{28}H_{39}NO_4$ (%) C, 74.14; H, 8.67; N, 3.09; Found C, 74.02; H, 8.62; N, 3.04.

Synthesis of butyl 4-(4′-(dodecyloxy)-2-hydroxybenzylideneamino)benzoate, C_{12}LH (1d)

Yield: 86%. IR (KBr, cm^{-1}): 3406 (−OH), 2959, 2923, 2846 (aliphatic C-H), 1712 (ester, C=O), 1627 (C = N), 1593, 1560 (Ph), 1278, 1234 (OPh); ^{1}H NMR (300 MHz, $CDCl_3$, 25°C) δ_H (ppm): 13.42 (s, 1H, −OH), 8.52 (s, 1H, −CH = N), 8.08 (d, J_1 (H,H) = 8.4 Hz, 2H, $-C_6H_4$), 7.30 (d, J_1 (H,H) = 8.2 Hz, 3H, $-C_6H_4$), 6.50 (d, 2H, $-C_6H_3$), 4.34 (t, 2H, $-OCH_2$), 4.04 (t, 2H, $COOCH_2$), 1.78-1.43 (m, 24H, $-[CH_2]_{12}$), 1.02 (t, 3H, $-CH_3$), 0.88 (t, 3H, $-CH_3$); ^{13}C NMR (75 MHz, $CDCl_3$, 25°C): δ_c 166.19, 164.10, 164.03, 162.74, 152.42, 133.85, 130.95, 128.11, 120.89, 112.73, 107.91, 101.57, 68.31, 64.85, 31.87, 30.77, 29.52, 29.29, 29.02, 25.95, 22.65, 19.27, 14.07, 13.75; Elemental analyses: calculated for $C_{30}H_{43}NO_4$ (%) C, 74.81; H, 9.01; N, 2.91; Found C, 74.73; H, 8.97; N, 2.93.

Synthesis of butyl 4-(4′-(tetradecyloxy)-2-hydroxybenzylideneamino)benzoate, $C_{14}LH$ (1e)

Yield: 85%. IR (KBr, cm^{-1}): 3409 (−OH), 2957, 2920, 2850 (aliphatic C-H), 1711 (ester, C=O), 1629 (C = N), 1591, 1563 (Ph), 1276, 1237 (OPh); ^{1}H NMR (300 MHz, $CDCl_3$, 25°C) δ_H (ppm): 13.43 (s, 1H, −OH), 8.54 (s, 1H, −CH = N), 8.10 (d, J_1 (H,H) = 8.4 Hz, 2H, $-C_6H_4$), 7.27 (d, J_1 (H,H) = 8.2 Hz, 3H, $-C_6H_4$), 6.49 (d, 2H, $-C_6H_3$), 4.33 (t, 2H, $-OCH_2$), 4.02 (t, 2H, $COOCH_2$), 1.80-1.43 (m, 28H, $-[CH_2]_{14}$), 1.01 (t, 3H, $-CH_3$), 0.89 (t, 3H, $-CH_3$); ^{13}C NMR (75 MHz, $CDCl_3$, 25°C): δ_c 166.17, 164.11, 164.04, 162.75, 152.40, 133.85, 130.94, 128.10, 120.89, 112.75, 107.89, 101.57, 68.31, 64.85, 31.87, 30.77, 29.52, 29.29, 29.02, 25.94, 22.65, 19.25, 14.07, 13.76; Elemental analyses: calculated for $C_{32}H_{47}NO_4$ (%) C, 75.40; H, 9.29; N, 2.75; Found C, 75.31; H, 9.23; N, 2.72.

Synthesis of butyl 4-(4′-(hexadecyloxy)-2-hydroxybenzylideneamino)benzoate, $C_{16}LH$ (1f)

Yield: 88%. IR (KBr, cm^{-1}): 3415 (−OH), 2960, 2922, 2849 (aliphatic C-H), 1715 (ester, C=O), 1626 (C = N), 1594, 1562 (Ph), 1275, 1235 (OPh); ^{1}H NMR (300 MHz, $CDCl_3$, 25°C) δ_H (ppm): 13.41 (s, 1H, −OH), 8.51 (s, 1H, −CH = N), 8.07 (d, J_1 (H,H) = 8.4 Hz, 2H, $-C_6H_4$), 7.28 (d, J_1 (H,H) = 8.2 Hz, 3H, $-C_6H_4$), 6.48 (d, 2H, $-C_6H_3$), 4.36 (t, 2H, $-OCH_2$), 4.01 (t, 2H, $COOCH_2$), 1.79-1.43 (m, 32H, $-[CH_2]_{16}$), 1.03 (t, 3H, $-CH_3$), 0.88 (t, 3H, $-CH_3$); ^{13}C NMR (75 MHz, $CDCl_3$, 25°C): δ_c 166.20, 164.10, 164.05, 162.76, 152.42, 133.85, 130.92, 128.12, 120.91, 112.74, 107.88, 101.58, 68.31, 64.84, 31.86, 30.77, 29.53, 29.29, 29.02, 25.95, 22.65, 19.25, 14.05, 13.74; Elemental analyses: calculated for $C_{34}H_{51}NO_4$ (%) C, 75.94; H, 9.56; N, 2.60; Found C, 75.84; H, 9.51; N, 2.63.

Copper(II) complex of butyl 4-(4′-(hexyloxy)-2-hydroxybenzylideneamino)benzoate, $(C_6L)_2Cu$ (2a)

To a solution of butyl 4-(4′-(hexyloxy)-2-hydroxybenzylideneamino)benzoate (0.80 g, 2 mmol) in 20 mL of hot methanol/chloroform (1/1,v/v) was added copper(II) acetate (0.20 g, 1 mmol) in 10 mL of methanol- and the mixture was stirred at room temperature for 4 h. The brown solid was filtered off, washed with methanol and recrystallized from chloroform/ethanol (1/1,v/v). All the other members of the series were prepared in a similar manner.

Yield: 76% (brown solid). IR (KBr, cm^{-1}): 2954, 2926, 2857 (aliphatic C-H), 1713 (ester, C=O), 1612 (C = N), 1594, 1530 (Ph), 1278, 1240 (OPh); UV–visible: λ_{max} = 436, 390, 278, 260, 208; Elemental analyses: calculated for $C_{48}H_{60}N_2O_8Cu$ (%) − C, 67.31; H, 7.06; N, 3.27, Cu, 7.42; Found C, 67.21; H, 7.02; N, 3.25, Cu, 7.40.

Copper(II) complex of butyl 4-(4′-(octyloxy)-2-hydroxybenzylideneamino)benzoate, $(C_8L)_2Cu$ (2b)

Yield: 78% (brown solid). IR (KBr, cm^{-1}): 2957, 2927, 2857 (aliphatic C-H), 1712 (ester, C=O), 1611 (C = N), 1593, 1531 (Ph), 1278, 1240 (OPh); UV–visible: λ_{max} = 442, 393, 282, 265, 212; Elemental analyses: calculated for $C_{52}H_{68}N_2O_8Cu$ (%) − C, 68.43; H, 7.51; N, 3.07, Cu, 6.96; Found C, 68.35; H, 7.46; N, 3.03, Cu, 6.92.

Copper(II) complex of butyl 4-(4′-(decyloxy)-2-hydroxybenzylideneamino)benzoate, $(C_{10}L)_2Cu$ (2c)

Yield: 80% (brown solid). IR (KBr, cm^{-1}): 2955, 2925, 2853 (aliphatic C-H), 1710 (ester, C=O), 1611 (C = N), 1591, 1535 (Ph), 1280, 1245 (OPh); UV–visible: λ_{max} = 432, 387, 280, 268, 209; Elemental analyses: calculated for $C_{56}H_{76}N_2O_8Cu$ (%) − C, 69.43; H, 7.91; N, 2.89, Cu, 6.56; Found C, 69.38; H, 7.93; N, 2.85, Cu, 6.53.

Copper(II) complex of butyl 4-(4′-(dodecyloxy)-2-hydroxybenzylideneamino) benzoate, $(C_{12}L)_2Cu$ (2d)

Yield: 77% (brown solid). IR (KBr, cm^{-1}): 2950, 2926, 2855 (aliphatic C-H), 1712 (ester, C=O), 1610 (C = N), 1602, 1538 (Ph), 1275, 1242 (OPh); UV–visible: $\lambda_{max} = 430, 391, 283, 262, 201$; Elemental analyses: calculated for $C_{60}H_{84}N_2O_8Cu$ (%) – C, 70.32; H, 8.26; N, 2.73, Cu, 6.20; Found C, 70.23; H, 8.20; N, 2.67, Cu, 6.14.

Copper(II) complex of butyl 4-(4′-(tetradecyloxy)-2-hydroxybenzylideneamino) benzoate, $(C_{14}L)_2Cu$ (2e)

Yield: 79% (brown solid). IR (KBr, cm^{-1}): 2952, 2924, 2851 (aliphatic C-H), 1714 (ester, C=O), 1612 (C = N), 1598, 1537 (Ph), 1282, 1241 (OPh); UV–visible: $\lambda_{max} = 438, 386, 279, 263, 207$; Elemental analyses: calculated for $C_{64}H_{92}N_2O_8Cu$ (%) – C, 71.11; H, 8.58; N, 2.59, Cu, 5.88; Found C, 71.02; H, 8.51; N, 2.53, Cu, 5.81.

Copper(II) complex of butyl 4-(4′-(hexadecyloxy)-2-hydroxybenzylideneamino) benzoate, $(C_{16}L)_2Cu$ (2f)

Yield: 75% (brown solid). IR (KBr, cm^{-1}): 2948, 2922, 2851 (aliphatic C-H), 1711 (ester, C=O), 1611 (C = N), 1601, 1540 (Ph), 1277, 1242 (OPh); UV–visible: $\lambda_{max} = 435, 392, 280, 261, 206$; Elemental analyses: calculated for $C_{68}H_{100}N_2O_8Cu$ (%) – C, 71.83; H, 8.86; N, 2.46, Cu, 5.59; Found C, 71.76; H, 8.80; N, 2.40, Cu, 5.52.

Acknowledgments

HKS (Senior Research Fellow) is grateful to Council of Scientific and Industrial Research (CSIR), New Delhi, India, for providing research fellowship. BS is grateful to DRDO, India (Project No. ERIP/ER/1203053/M/01/1542) for financial assistance. The authors wish to thank Dr. Sandeep kumar and Ms. Vasuda, Raman Research Institute, Bangalore, India for the XRD analysis.

References

[1] Hird, M. (2011). *Liq. Cryst.*, *38*, 11–12, 1467.
[2] Teucher, I., Paleos, C. M., & Labes, M. M. (1970). *Mol. Cryst. Liq. Cryst.*, *11*, 187.
[3] Hoshino, N. (1998). *Coord. Chem. Rev.*, *174*, 77.
[4] (a) Giroud-Godquin, A. M., & Maitlis, P. M. (1991). *Angew. Chem. Ed. Eng.*, 30, 375. (b) Espinet, P., Esteruelas, M. A., Oro, L. A., Serrono, J. L., & Sola, E. (1992). *Coord. Chem. Rev.*, *117*, 215. (c) Polishchuk, A. P., & Timofeeva, T. V. (1993). *Russ. Chem. Rev.*, *62*, 291. (d) Hudson, S. A., & Maitlis, P. M. (1993). *Chem. Rev.*, *93*, 861. (e) Serrano, J. L. (Ed.) (1996). In. *Metallomesogens: Synthesis, Properties and Applications*, Wiley-VCH: Weinheim. (f) Bruce, D. W. (1996). In. *Inorganic Materials*, Bruce, D. W. & O'Hare, D. (Eds.), 2nd Edn., Wiley, Chichester: 429–552. (g) Giroud-Godquin, A. M. (1998). In *Handbook of Liquid Crystals*, Vol. 2B, Demus, D., Goodby, J., Gray, G. W., Spiess, H. W., & Vill, V. (Eds.), Chap. XIV, Wiley VCH: Weinheim. (h) Donnio, B., & Bruce, D. W. (1999). *Struct. Bonding*, *95*, 193. (i) Prajapati, A. K., & Bonde, N. (2006). *Mol. Cryst. Liq. Cryst.*, *33*, 1189.
[5] Galyametdinov, Yu. G., Ovchinnikov, I. V., Bolotin, B. M., Etingen, N. B., Ivanova, G. I., & Yagfarova, L.M. (1984). *Izv. Akad. SSSR, Ser. Khim.*, *10*, 2379.
[6] Bikchantaev, I. G., Galyametdinov, Yu. G., & Ovchinnikov, I. V. (1987). *Zh. Strukt. Khim.*, *28*, 61.
[7] Ovchinnikov, I. V., Bikchantaev, I. G., Galyametdinov, Yu. G., & Galimov, R. M. (1988). *24th Ampere congress, Poznan.*
[8] Ovchinnikov, I. V., Galyametdinov, Yu. G., & Bikchantaev, I. 0. (1989). *Izv. Akad. Nuuk SSSR Ser. Fiz.*, *53*, 1870.
[9] Caruso, U., Roviello, A., & Sirigu, A. (1988). *Liq. Cryst.*, *3*, 1515.

[10] (a) Singh, B., Singh, M. K., Dhar, R., & Srivastava, A. K. (2004). *Mol. Cryst. Liq. Cryst.*, *411*, 29. (b) Singh, H. K., Singh, S. K., Kumar, V., & Singh, B. (2013). *Mol. Cryst. Liq. Cryst. 587*, 1.

[11] Galewaki, Z. (1994). *Mol. Cryst. Liq. Cryst.*, 249, 43.

[12] Weisberger, A., & Praskver, F. S. (1956). *Organic Solvents*, International Publishers Inc.: New York, 1263.

[13] Frisch, M. J., et al. (2003). In *Gaussian 03, Revision A.1*, Gaussian, Inc.: Pittsburgh.

[14] Hohenberg, P., & Kohn, W. (1964) *Phys. Rev. B*, 136, 864.

[15] Kohn, W., & Sham, L. J. (1965). *Phys. Rev. A*, *140*, 1133.

[16] Becke, A. D. (1988). *Phys. Rev. A*, *38*, 3098.

[17] Becke, A. D. (1992). *J. Chem. Phys.*, *96*, 2155.

[18] Becke, A. D. (1992). *J. Chem. Phys.*, *97*, 9173.

[19] Becke, A. D. (1993). *J. Chem. Phys.*, *98*, 5648.

[20] Lee, C., Yang, W., & Parr, R. G. (1988). *Phys. Rev. B*, 37, 785.

[21] Ditchfield, R., Hehre, W. J., & Pople, J. A. (1971). *J. Chem. Phys.*, *54*, 724.

[22] Hehre, W. J., Ditchfield, R., & Pople, J. A. (1972). *J. Chem. Phys.*, *56*, 2257.

[23] Dziembowska, T. et al. (2003). *J. Spectrochim. Acta Part A*, *59*, 2175.

[24] Dennington II, R., Keith, T., Millam, J., Eppinnett, K., Hovell, W. L., Gilliland, R. (2003). *Gauss View 03*, Semichem, Inc.: Shawnee Mission, KS.